

ORIGINAL RESEARCH

# Resveratrol Delays Diabetic Cardiomyopathy Fibrosis by Regulating Mitochondrial Autophagy

Liqun Yang, MD; Zhe Gao, PhD; Hang Zhao, PhD; Zhimei Zhang, PhD; Guangyao Song, PhD

## ABSTRACT

**Objective** • To explore whether resveratrol can postpone the fibrosis associated with diabetic cardiomyopathy (DCM) by modulating the mitochondrial autophagy response through the AMPK/SIRT1-mediated IRE1 $\alpha$ /PINK signaling pathway.

**Methods** • A DCM mouse model was established using a high-sugar high-fat diet and streptozotocin. Resveratrol was administered to a subset of the DCM mouse models for comparison. Echocardiography, Masson staining, TNUEL assay, and transmission electron microscopy were employed to evaluate the cardiac status, myocardial fibrosis, myocardial cell apoptosis, and morphological changes of myocardial cells and their internal mitochondria in each group of mice. Western blot staining was performed on myocardial tissues to assess the protein expression levels of p-AMPK, SIRT1, SIRT3, p22, GP91, p-IRE1 $\alpha$ , XBP1s, PINK, Parkin, LC3I, and Beclin. Mouse myocardial cells were cultured *in vitro* and intervened with a high-sugar high-fat diet, resveratrol, and GSK690693 (an AMPK inhibitor) to observe the protein expression levels of p-AMPK, p22, XBP1s, and PINK in mouse myocardial cells in each group.

**Results** • Results from echocardiography, Masson staining, TNUEL assay, and transmission electron microscopy showed

that resveratrol administration alleviated cardiac damage, myocardial fibrosis, myocardial cell apoptosis, and mitochondrial autophagy in DCM mice. Resveratrol administration promoted the expression of phosphorylated AMP-activated protein kinase (p-AMPK), sirtuin 1 (SIRT1), and sirtuin 3 (SIRT3) in the myocardial tissue of mice, while lowering the elevated protein expression levels of p22 subunit (p22), guanine nucleotide-binding protein q polypeptide 1 (GP91), phosphorylated inositol-requiring enzyme 1 alpha (p-IRE1 $\alpha$ ), X-box binding protein 1 spliced form (XBP1s), PTEN-induced putative kinase 1 (PINK), Parkin, microtubule-associated proteins light chain 3 isoform I (LC3I), and Beclin (Bcl-2 interacting protein) caused by DCM. GSK690693 (an AMPK inhibitor) suppressed the expression of p-AMPK, SIRT1, and SIRT3 and enhanced the protein expression of p22, XBP1s, and PINK.

**Conclusion** • Resveratrol postpones dilated cardiomyopathy fibrosis by regulating the mitochondrial autophagy response through the AMP-activated protein kinase (AMPK)/silent mating type information regulation 2 homolog 1 (SIRT1)-mediated inositol-requiring enzyme 1 alpha (IRE1 $\alpha$ )/PTEN-induced putative kinase 1 (PINK) signaling pathway. (*Altern Ther Health Med.* 2025;31(1):143-149).

**Liqun Yang, MD; Guangyao Song, PhD**, Department of Internal Medicine; Hebei Medical University; Department of Endocrinology; Hebei General Hospital; Shijiazhuang; People's Republic of China. **Zhe Gao, PhD; Hang Zhao, PhD; Zhimei Zhang, PhD**, Department of Endocrinology; Hebei General Hospital; Shijiazhuang; People's Republic of China.

Corresponding author: Guangyao Song, PhD

E-mail: [sguangyao2@163.com](mailto:sguangyao2@163.com)

## INTRODUCTION

Diabetic cardiomyopathy (DCM) is a cardiac structural and functional abnormality that exists in diabetic patients without coronary heart disease, hypertension, heart valve

disease, and other conditions.<sup>1</sup> DCM is mainly characterized by myocardial apoptosis, interstitial fibrosis, and left ventricular diastolic and systolic dysfunction.<sup>2</sup> DCM is a major cause of sudden cardiac death and death in diabetic patients,<sup>3</sup> so the prevention and treatment of DCM are necessary. The pathogenesis of DCM is currently unclear, and mitochondrial autophagy-induced cardiac tissue fibrosis is the main risk factor for DCM progression.<sup>4</sup> Inhibiting mitochondrial autophagy may be an effective treatment for improving heart function. Hyperglycemia and hyperlipidemia are the initiating factors of abnormal myocardial metabolism in diabetic cardiomyopathy, and mitochondria are an important regulator of energy supply and the main source of reactive oxygen species (ROS) in the body. High glucose directly or indirectly leads to electron transport chain obstruction, oxidative

phosphorylation disorders, reduced Adenosine Triphosphate (ATP) synthesis, and further increases ROS production. A vicious circle is formed, amplifying the effect.<sup>5</sup> In some studies, it has been found that increasing ROS and reducing mitochondrial membrane potential (MMP) damage the mitochondrial function and ATP synthesis and then activate the adenosine monophosphate-activated protein kinase/mammalian target of rapamycin (AMPK/mTOR) autophagy signaling pathway. Further experiments have proved that excessive mitochondrial autophagy can promote cell death through the ROS-ATP-AMPK signaling pathway.<sup>6</sup>

Resveratrol is the first polyphenolic natural product found to activate Sirtuin 1 (SIRT1) activity. It has various physiological activities such as anti-inflammatory, anti-tumor, antioxidant, and estrogen-like effects.<sup>7</sup> Resveratrol is a plant toxin and antioxidant widely found in fruits, traditional Chinese medicine, and wine, and exhibits cardiovascular protective effects. It is the strongest SIRT1 activator discovered so far.<sup>8</sup> SIRT1 regulates cell differentiation, metabolism, aging, and apoptosis by deacetylating proteins.<sup>9</sup> SIRT1 and its activator resveratrol have positive effects on extending cell lifespan, antioxidation, apoptosis, energy metabolism, inflammation, and autophagy.

## MATERIALS AND METHODS

### Animal modeling and grouping

The study utilized a cohort of 24 male C57BL/6J mice, aged between 6 and 8 weeks, with a weight range of 22-26 g. These mice were procured from Henan Scubio Biotechnology Co., LTD., and housed under controlled conditions at an ambient temperature of 20-25°C and relative humidity of 40% to 70%. The animals were randomly divided into the control group (n = 8), DCM group (n = 8), and DCM plus resveratrol group (n = 8). The DCM group received a high-sugar and high-fat diet (20% sucrose, 10% lard, and a basic diet); after 12 hours of fasting on the fourth and fifth weeks, the mice were given two intraperitoneal injections of 1% streptozotocin (30 mg/kg, STZ). The STZ solution was used and prepared on the same day. The control group was fed a normal diet and received an equal amount of citrate buffer by intraperitoneal injection at the same time. The DCM plus resveratrol group received an intravenous injection of resveratrol at a dose of 30 mg/kg/d based on the DCM group. After 72 hours, fasting blood glucose levels were measured by collecting tail vein blood. Mice with blood glucose levels above 16.7 mmol/L for two consecutive times were included in the DCM group, while those whose blood glucose levels did not reach the mentioned standard level were excluded. The mice were fed for an additional 10 weeks. The mice continued to be fed the high-sugar and high-fat diet for another 8 weeks before sacrificing four randomly selected individuals for observation of myocardial structure changes compared to normal healthy mice of the same age group.

### Echocardiography to assess cardiac function in mice

At the conclusion of a four-week duration subsequent to the administration of the last inoculation, an assessment of

cardiac functionality was meticulously conducted for all murine subjects. This evaluation was facilitated by the employment of the Vevo 2100, a sophisticated imaging apparatus tailored for diminutive creatures. During the examination, the rodents were subjected to an inhalation of isoflurane at a concentration of 20 mL/L to induce a state of anesthesia, thereafter they were delicately positioned in a dorsal recumbent attitude upon the surgical platform. The echographic transducer was meticulously maneuvered to secure lucid bidimensional representations of both the short-axis and long-axis perspectives of the left cardiac ventricle. Trios of cardiac cycles, in succession, were duly recorded and the mean values therefrom calculated, in both long-axis and short-axis M-modes, with the objective of delineating various parameters. These parameters comprised the left ventricular end-diastolic internal diameter, zenith and nadir pressure deltas, as well as the maximal velocities of left ventricular pressure augmentation and diminution, in conjunction with the fraction of contraction.

### Animal sampling and sample collection

All surviving mice were euthanized by bleeding from the carotid artery after inhalation of 30 mL/L isoflurane anesthesia. To minimize pain and stress during the euthanasia process, the mice were continuously anesthetized with 20 mL/L isoflurane via nasal inhalation. PBS was used to flush the heart from both the left and right atria at the base of the heart using a 1 mL syringe. After flushing, the heart was quickly placed on a filter paper, the left and right atria, right ventricle, and interventricular septum were removed, and the left ventricular part was transferred to a 1.5 mL Eppendorf tube, rapidly frozen in liquid nitrogen, and stored in a -80°C freezer for later use. The remaining part of the heart was flushed with 40 mL/L paraformaldehyde solution, fixed in 40 mL/L paraformaldehyde solution for 24 hours, and embedded in paraffin or frozen for sectioning.

### Masson staining

Take 4 µm thick slices of heart tissue, dewax them, wash them with distilled water, add Bouin's fixative, and place them in a water bath, raising the temperature from room temperature to 56°C for 15 minutes. Thoroughly rinse with water, add Masson's trichrome acid fuchsin solution for 5-10 minutes, wash with distilled water; differentiate with 1% phosphomolybdic acid water solution for 3-5 minutes; air dry, directly stain with aniline blue solution for 5-10 minutes, wash with distilled water; immerse in 0.2% acetic acid water solution for a while, dehydrate with 95% ethanol, absolute ethanol, xylene, and mount with neutral gum. Take pictures under a microscope using a 1.25× objective, and determine the degree of fibrosis by analyzing the average ratio of fibrotic area to left ventricular area using Image J software.

### Terminal deoxynucleotidyl transferase-mediated dUTP nick end labeling (TUNEL) assay

Place heart tissue slices in xylene for two washes, 5 minutes each time; wash with absolute ethanol twice, 3

minutes each time; wash with 95% and 75% ethanol once each, 3 minutes each time; and finally wash with PBS for 5 minutes. Add proteinase K solution (20 µg/ml) to digest the washed tissue slices at room temperature for 15 minutes; rinse with distilled water 4 times, 2 minutes each time; add PBS containing 2% hydrogen peroxide to the staining dish and react at room temperature for 5 minutes; then wash with PBS twice, 5 minutes each time; remove excess liquid with filter paper, add TdT enzyme buffer to the slices, and incubate at room temperature for 5 minutes; remove excess liquid with filter paper, add 54 µl of TdT enzyme reaction solution to the slices, and react at 37°C in a humid box for 1 hour; place the slices in a staining dish, add preheated 37°C wash and stop reaction buffers, keep warm for 30 minutes, gently shake the slices once every 10 minutes; rinse the tissue slices with PBS 3 times, 5 minutes each time, directly add anti-fluorescence quenching mounting medium on the slices, observe and take pictures to calculate the apoptosis rate. Myocardial cell apoptosis rate = [number of apoptotic cells/total number of cells] × 100%.

Western blot to detect the protein expression of p-AMPK, SIRT1, SIRT3 p22, GP91, p-IRE1α, PINK, Parkin, LC3I, Beclin, and XBP1s in mouse myocardial cells of each group.

On the ice, perform the following operations: Take approximately 100 mg of mouse myocardial tissue from each group, chop it, and place it in 1000 µl RIPA lysis buffer (containing 10 µl PMSE, 10 µl NaF, and 10 µl Na<sub>3</sub>VO<sub>4</sub>). After homogenizing carefully, let it stand for 30 minutes at 4°C, centrifuge at 12000 rpm for 5 minutes, and collect the supernatant. Measure the total protein concentration of the tested samples using the Bicinchoninic acid (BCA) method. Prepare SDS-polyacrylamide gel and add 2.5 µl pre-stained protein marker to the first well. Mix the extracted protein samples with 5× loading buffer (volume ratio of 1:4), boil at 95°C for 5 minutes, and then cool down and load them into the wells. The loading amount is 100 µg per well. Perform electrophoresis until the marker bands separate and the bromophenol blue reaches the bottom of the separating gel. After electrophoresis, remove the gel, trim it according to the protein molecular weight indicated by the marker, place a slightly larger polyvinylidene difluoride (PVDF) membrane between double-layer filter paper and sponge pad, remove bubbles, and put it in a pre-cooled electrophoresis tank at 4°C, 220 mA. Put the PVDF membrane in a plastic bag, add 5% skimmed milk powder, shake gently at room temperature for 2 hours on a shaker, then remove the PVDF membrane, wash it with TBST solution for 10 minutes × 3 times, incubate the PVDF membrane in a diluted primary antibody solution at 4°C overnight, perform washing, put the PVDF membrane in TBST-diluted HRP-labeled secondary antibody, shake gently at room temperature for 2 hours, and then wash again. Perform chemiluminescent detection and imaging using an imaging system. Use the Quantity One software system.

### Transmission Electron Microscopy

Subsequent to a 24-hour immersion in a 2.5% glutaraldehyde solution, the samples were gently washed with

0.1 mol/L Sorensen's phosphate buffer. The specimens were subsequently subjected to a secondary fixation in a 1% osmium tetroxide-phosphate buffer for an interval ranging from 1.5 to 2.0 hours and maintained at a frigid 4 degrees Celsius. A tiered dehydration procedure was employed, utilizing acetone concentrations of 50%, 75%, and 90%, each stage lasting for a quarter-hour at a consistent 4 degrees Celsius, proceeded by a trio of decadic-minute exposures to anhydrous acetone at ambient temperature. Following the exhaustive amalgamation of Epon812 embedding resin and the meticulous expulsion of any gaseous occlusions, the specimens were subjected to a 12-hour infiltration at controlled room temperature, intermittently agitated, and subsequently solidified over the course of 48 hours at an elevated temperature of 60 degrees Celsius. The embedding blocks were trimmed, and semi-thin sections of 10 µm were cut using a glass knife on an ultramicrotome. After softening with 1% sodium hydroxide in absolute ethanol for 15 minutes, the sections were rinsed and stained with methylthionine chloride and basic fuchsin for optical observation and localization. Ultrathin sections were subsequently prepared with an ultramicrotome, and double staining with uranyl acetate and lead citrate was performed for electron microscope observation and photography.

### Beclin Cell culture and grouping

HL-1 cells were cultured in DMEM containing 10% fetal bovine serum (with 25 mmol/L glucose) and passaged normally. The experimental groups were as follows: normal control group (group 1), resveratrol group (group 2), high glucose (HG) group (group 3), resveratrol plus HG group (group 4), HG plus GSK690693 (AMPK inhibitor) group (group 5), and HG plus resveratrol plus GSK690693 group (group 6). All drugs in each group were prepared with DMEM containing 10% fetal bovine serum. The concentration of high glucose was 40 mmol/L, and the concentration of resveratrol was 100 µmol/L. The relevant tests were conducted 24 hours after drug administration.

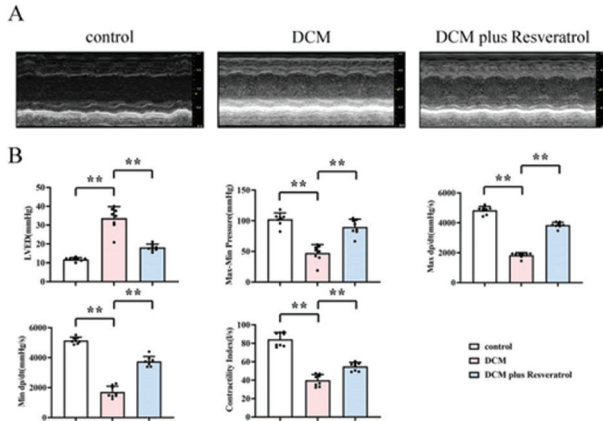
### Western blot analysis of p-AMPK, p22, XBP1, and PINK protein expression

Collect the co-cultured myocardial cells from each group, extract total proteins using a kit, quantify the proteins, separate them by electrophoresis, transfer them to PVDF membranes, and incubate with primary antibodies overnight at 4°C. After incubation with secondary antibodies at 37°C for 90 minutes, the membranes were developed, and the band intensities were measured using Image J software to calculate the relative protein expression.

### Statistical analysis

All experiments were organized and analyzed using SPSS 22.0 software. Continuous variables were presented as mean ± standard deviation ( $\bar{x} \pm s$ ). Comparison between two groups was performed using a *t* test, while comparison among multiple groups was performed using one-way ANOVA. *P* < .05 was considered statistically significant.

**Figure 1.** Observation (A) and Statistics (B) of Mouse Heart Conditions by Echocardiography



**RESULTS**

Echocardiography was used to assess the cardiac status of the different groups of mice. The results showed that, compared to the control group, the DCM group had a significant increase in left ventricular end-diastolic (LVED) diameter ( $P < .01$ ), as well as a significant decrease in maximal-minimal pressure difference, maximum rate of pressure rise and fall, and fractional shortening ( $P < .01$ ). The DCM plus resveratrol group had a significant decrease in LVED diameter compared to the DCM group ( $P < .05$ ), as well as a significant increase in the maximal-minimal pressure difference, the maximum rate of rise and fall in pressure, and the fractional shortening ( $P < .05$ ). See Figure 1 for details.

**Masson’s trichrome staining**

The results showed that the control group had very little blue-stained area in the myocardial tissues, mainly showing overall red staining, indicating a very low degree of fibrosis under normal conditions. Compared to the control group, the DCM group had a significant increase in blue-stained area in the cardiac tissues, indicating a significant increase in fibrosis ( $P < .01$ ). The DCM plus resveratrol group had a significant decrease in blue-stained area in the cardiac tissues compared to the DCM group, which indicates a significant reduction in fibrosis ( $P < .05$ ). This suggests that resveratrol can effectively inhibit the fibrosis of cardiac tissues caused by DCM. See Figure 2A for details.

**Terminal deoxynucleotidyl transferase-mediated dUTP nick-end labeling (TUNEL) assay**

The results showed that in the cardiac tissues of the control group mice, there were very few brown-stained positive cells, and apoptotic cells were rare. Compared to the control group, the DCM group showed a significant increase in the number of brown-stained positive cells in the cardiac tissues, indicating a significant increase in apoptosis ( $P < .01$ ). The DCM plus resveratrol group showed a significant decrease in the number of brown-stained positive cells compared to the DCM group, indicating a reduction in apoptosis caused by DCM ( $P < .05$ ). See Figure 2B for details.

**Figure 2.** Observation and Statistical Analysis of (A) Mouse Heart Fibrosis by Masson Staining and (B) Mouse Myocardial Cell Apoptosis by TUNEL Detection

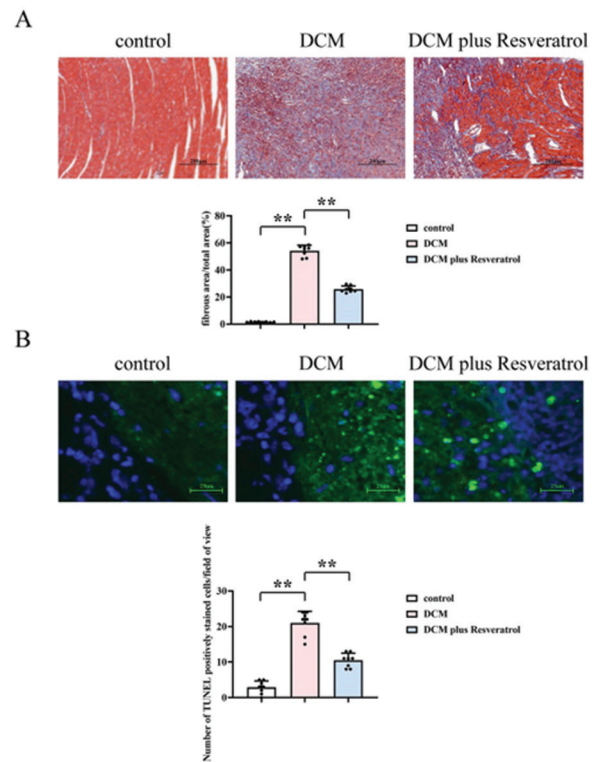
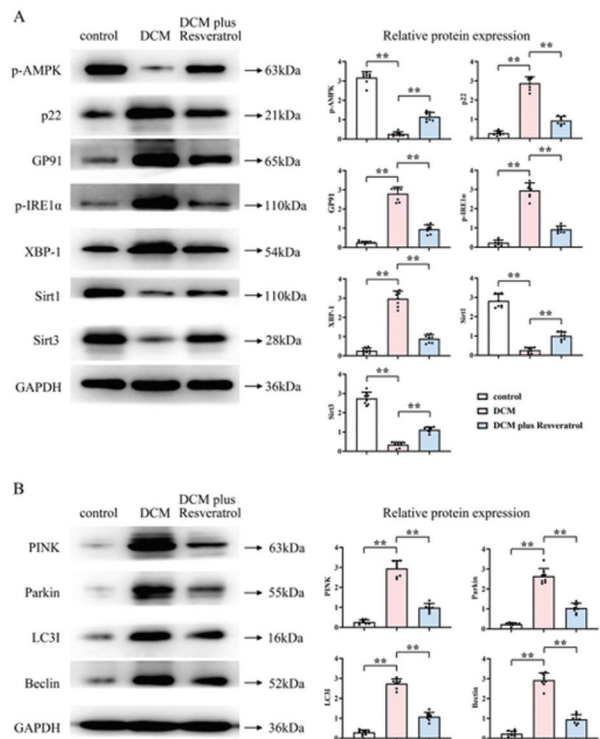


**Figure 3.** Results of Western Blot Detection. (A) Detection of p-AMPK, SIRT1, p22, GP91, p-IRE1α, XBP1s, PINK, Parkin, LC3I, and Beclin Protein Expression in Mouse Myocardial Cells by Western Blot. (B) Statistical Analysis of Western Blot Results.



### Western blot analysis

The results showed that, compared to the control group, the DCM group had a significant reduction in the protein expression levels of p-AMPK, SIRT1, and SIRT3, and had a significant increase in the protein expression levels of p22, GP91, p-IRE1 $\alpha$ , XBP1s PINK, Parkin, LC3I, and Beclin (Figure 3A,  $P < .01$ ). Compared to the DCM group, the DCM plus resveratrol group had a significant increase in the protein expression levels of p-AMPK, SIRT1, and SIRT3, and had a significant reduction in the protein expression levels of p22, GP91, p-IRE1 $\alpha$ , XBP1s PINK, Parkin, LC3I, and Beclin (Figure 3B,  $P < .05$ ).

### Transmission electron microscopy

The results showed that in the control group, the cardiac myocytes had a normal arrangement, with normal mitochondrial morphology and ridge arrangement. In the DCM group, there was a significant amount of cardiac myocyte rupture, disappearance, and reduction of mitochondrial ridges. In the DCM plus resveratrol group, there were some cardiac myocyte ruptures, as well as fractured mitochondrial ridges and reduced quantity. See Figure 4A for details.

### p-AMPK, SIRT1, SIRT3, p22, XBP-1, and PINK protein expression

The Western blot results showed that there were no significant differences in the expression levels of p-AMPK, SIRT1, SIRT3, p22, XBP-1, and PINK proteins between Group 1 and Group 2 ( $P > .05$ ). Compared to Group 3, the expression of p-AMPK, SIRT1, and SIRT3 protein was significantly increased in Group 4 ( $P < .05$ ), while the expression levels of p22, XBP-1, and PINK proteins were significantly decreased ( $P < .05$ ). Compared to Group 5, there were no significant differences in the expression levels of p-AMPK, SIRT1, SIRT3, p22, XBP-1, and PINK proteins in Group 6 ( $P > .05$ ), but compared to Groups 3 and 4 without added AMPK inhibitor, the expression levels of p-AMPK, SIRT1, SIRT3, protein were significantly decreased in Groups 5 and 6 ( $P < .05$ ), while the expression levels of p22, XBP-1, and PINK proteins were significantly increased ( $P < .05$ ), as shown in Figure 5.

### DISCUSSION

Diabetic cardiomyopathy (DCM) is a common complication in patients with diabetes, which greatly increases the incidence of heart failure in diabetic patients.<sup>10</sup> The vicious cycle of increased oxidative stress due to hyperglycemia and hyperlipidemia in diabetes, leading to enhanced mitochondrial autophagy and amplified endoplasmic reticulum (ER) stress, further aggravates the progression of diabetic cardiomyopathy. Autophagy plays an important role in maintaining cardiac function and morphology by clearing dysfunctional organelles and protein aggregates.<sup>11</sup> Therefore, when the process of autophagy is disrupted, protein imbalance can occur and contribute to the development of cardiac-related diseases.<sup>12</sup>

**Figure 4.** Results of Electron Microscopy and Western Blot Detection. (A) Observation of Mouse Myocardial Cells and Mitochondria by Electron Microscopy and (B) Expression and Statistical Analysis of PINK, Parkin, LC3I, and Beclin Proteins in Mouse Myocardial Cells by Western Blot.

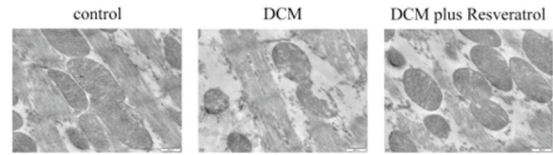


**Figure 5.** Results of Western Blot Detection of p-AMPK, SIRT1, SIRT3, p22, XBP1, and PINK Protein Expression in Different Groups of Cultured Myocardial Cells

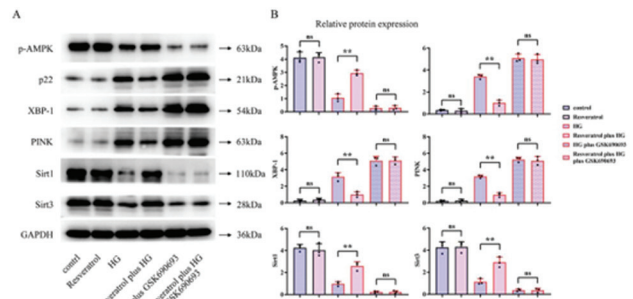
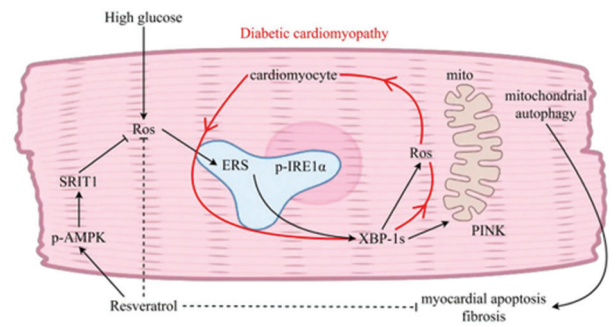


**Figure 6.** Resveratrol has the ability to postpone the fibrosis of diabetic cardiomyopathy by controlling the mitochondrial autophagy response through the AMPK/SIRT1-mediated IRE1 $\alpha$ /PINK signaling pathway.



Mitochondrial autophagy is the process of degrading abnormal or excess mitochondria in cells to correct mitochondrial dysfunction, improve mitochondrial quality, and maintain cardiac homeostasis.<sup>13</sup> Under physiological conditions, mitochondrial autophagy exerts a protective effect by removing damaged mitochondria. In the pathological context of DCM, the regulation of mitochondrial autophagy becomes complex. When mitochondrial autophagy is inhibited, insufficient clearance of abnormal mitochondria leads to excessive accumulation of ROS, triggering myocardial cell death. On the other hand, excessive activation of mitochondrial autophagy results in excessive clearance of mitochondria that cannot meet the energy supply for the myocardium. Several aspects of mitochondrial physiology, including biogenesis, transport, and recruitment of

autophagic components, are concentrated in the PINK1-Parkin pathway.<sup>14</sup>

In diabetes, the regulatory role of p-AMPK (phosphorylated AMPK) is crucial. Diabetes is a metabolic disorder characterized by impaired insulin secretion or action in the body, leading to elevated blood sugar levels. In individuals with diabetes, there is often a reduction in the active state of AMPK. This could be attributed to an increase in intracellular ATP levels during hyperglycemia, which subsequently inhibits AMPK activation. Diminished AMPK activity may disrupt glucose metabolism by decreasing glucose uptake and utilization while promoting excessive glucose production and fatty acid synthesis.<sup>19</sup>

SIRT1, a pivotal NAD<sup>+</sup>-dependent deacetylase, has been implicated in the pathogenesis of diabetes mellitus, a metabolic disorder characterized by aberrant insulin secretion or action leading to elevated blood glucose levels. SIRT1 exerts crucial regulatory control over glucose metabolism by modulating various signaling pathways and transcription factors associated with this process. Its activation enhances insulin signaling, and facilitates glucose uptake and utilization, while suppressing hepatic gluconeogenesis and glycogenolysis, thereby effectively reducing hyperglycemia. Furthermore, SIRT1 also plays a pivotal role in maintaining energy homeostasis and regulating insulin secretion through its involvement in fatty acid oxidation, gluconeogenesis regulation, and energy metabolism modulation among other processes that collectively influence energy balance and insulin resistance.<sup>20</sup>

X-box binding protein 1 (XBP1) is a crucial transcription factor that has been implicated in the pathogenesis of diabetes, a metabolic disorder characterized by hyperglycemia and impaired insulin secretion or action. XBP1 serves as a key regulator of endoplasmic reticulum (ER) stress response, which plays a pivotal role in modulating cellular responses to ER stress. In the context of diabetes, elevated levels of ER stress are often observed in pancreatic beta cells and other tissues, which is potentially attributed to dysregulation of glucose metabolism, oxidative stress, and lipid metabolism abnormalities. By governing gene transcription involved in the ER stress response pathway, XBP1 exerts a significant influence on cellular adaptation to stress and metabolic regulation. Notably, it has been demonstrated that XBP1 plays an essential protective role in pancreatic beta cells by regulating intracellular insulin biosynthesis and secretion while preserving their functional integrity.<sup>21</sup>

GP91 is a component of nicotinamide adenine dinucleotide phosphate (NADPH) oxidase, which has been implicated in the pathogenesis of diabetes. NADPH oxidase is an enzyme responsible for generating reactive oxygen species within cells. Diabetes is a metabolic disorder characterized by elevated blood glucose levels resulting from abnormal insulin secretion or action. Insulin resistance and inflammatory response are considered crucial pathological processes contributing to tissue and organ damage during diabetes progression. GP91 plays a significant role in the development and advancement of

diabetes, as evidenced by significantly increased expression of its subunit within diabetic tissues and organs. The upregulation of the GP91 subunit promotes the production of ROS, thereby augmenting cellular oxidative stress levels, leading to insulin resistance and cellular injury.<sup>22</sup> PINK1, a serine/threonine protein kinase mainly present in the outer membrane of mitochondria, accumulates on the outer membrane of mitochondria when mitochondrial membrane potential is reduced, proteolytic enzyme activity decreases, and degradation of PINK1 is reduced, forming a high molecular weight complex that includes components of the translocase of the outer membrane (TOM) complex, thereby facilitating the recruitment of Parkin.<sup>15</sup> ROS is mainly produced in mitochondria. Under normal conditions, ROS can be eliminated by endogenous antioxidant systems, thus reducing the level of ROS. Oxidative stress refers to the state of tissue damage caused by the imbalance between oxidation and antioxidant systems when the body is exposed to various harmful stimuli. During oxidative stress, the generation of ROS exceeds its clearance capacity, which can damage mitochondrial function. Therefore, timely clearance of dysfunctional mitochondria to inhibit ROS production may be a more effective therapeutic approach for treating myocardial damage in DCM.<sup>16</sup> Studies have shown that ER stress can promote the phosphorylation of IRE1 $\alpha$  and increase the secretion of X-box binding protein 1 activated form (XBP1s).<sup>17</sup> The XBP1s plays a critical role in promoting the PINK1/Parkin pathway in cardiac myocytes, and the PINK1/Parkin pathway promotes mitochondrial autophagy in cardiac myocytes. Excessive mitochondrial autophagy can lead to myocardial cell apoptosis and promote cardiac fibrosis.<sup>18</sup>

In this study, it was found that in the DCM mouse model treated with resveratrol, the phosphorylation level of AMPK and the expression of SIRT1 protein increased, while the expression of oxidative stress marker p22 decreased significantly compared to the DCM model group. These results indicate that resveratrol can activate AMPK phosphorylation and increase the expression of SIRT1, thereby increasing the level of antioxidant enzymes, reducing ROS levels, reducing the damaging effects of ROS on cardiac mitochondria, and playing an important role in maintaining cellular redox homeostasis, thus protecting the myocardium. The reduction of excessively elevated levels of oxidative stress caused by DCM acts as a brake on the vicious cycle of DCM, leading to a decrease in ER stress level, a decrease in XBP1s secretion level, and a subsequent decrease in mitochondrial autophagy level. This ultimately helps to decrease myocardial cell apoptosis and reduce myocardial tissue fibrosis, thereby delaying the progression of diabetic cardiomyopathy.

## CONCLUSION

In essence, resveratrol has the potential to retard the fibrotic progression of diabetic cardiomyopathy by modulating the mitochondrial autophagic response through the AMPK/SIRT1-mediated IRE1 $\alpha$ /PINK signaling cascade.

## AUTHOR DISCLOSURE STATEMENT

There has been no disclosure of any potential conflicts of interest that might influence the outcomes of the research.

## ACKNOWLEDGEMENT

The authors would like to thank all individuals who participated in the experiment.

## FUNDING

The research received no funding of any kind.

## REFERENCES

1. Ritchie RH, Abel ED. Basic Mechanisms of Diabetic Heart Disease. *Circ Res*. 2020;126(11):1501-1525. doi:10.1161/CIRCRESAHA.120.315913
2. Tan Y, Zhang Z, Zheng C, Wintergerst KA, Keller BB, Cai L. Mechanisms of diabetic cardiomyopathy and potential therapeutic strategies: preclinical and clinical evidence. *Nat Rev Cardiol*. 2020;17(9):585-607. doi:10.1038/s41569-020-0339-2
3. Jia G, Whaley-Connell A, Sowers JR. Diabetic cardiomyopathy: a hyperglycaemia- and insulin-resistance-induced heart disease. *Diabetologia*. 2018;61(1):21-28. doi:10.1007/s00125-017-4390-4
4. Zheng D, Chen L, Li G, et al. Fucoxanthin ameliorated myocardial fibrosis in STZ-induced diabetic rats and cell hypertrophy in HG-induced H9c2 cells by alleviating oxidative stress and restoring mitophagy. *Food Funct*. 2022;13(18):9559-9575. doi:10.1039/D2FO01761J
5. Boudina S, Abel ED. Mitochondrial uncoupling: a key contributor to reduced cardiac efficiency in diabetes. *Physiology (Bethesda)*. 2006;21(4):250-258. doi:10.1152/physiol.00008.2006
6. Zhang K, Zhou X, Wang J, et al. Dendrobium officinale polysaccharide triggers mitochondrial disorder to induce colon cancer cell death via ROS-AMPK-autophagy pathway. *Carbohydr Polym*. 2021;264:118018. doi:10.1016/j.carbpol.2021.118018
7. Hou X, Rooklin D, Fang H, Zhang Y. Resveratrol serves as a protein-substrate interaction stabilizer in human SIRT1 activation. *Sci Rep*. 2016;6(1):38186. doi:10.1038/srep38186
8. Howitz KT, Bitterman KJ, Cohen HY, et al. Small molecule activators of sirtuins extend *Saccharomyces cerevisiae* lifespan. *Nature*. 2003;425(6954):191-196. doi:10.1038/nature01960
9. Giannakou ME, Partridge L. The interaction between FOXO and SIRT1: tipping the balance towards survival. *Trends Cell Biol*. 2004;14(8):408-412. doi:10.1016/j.tcb.2004.07.006
10. Chen L, Magliano DJ, Zimmet PZ. The worldwide epidemiology of type 2 diabetes mellitus—present and future perspectives. *Nat Rev Endocrinol*. 2011;8(4):228-236. doi:10.1038/nrendo.2011.183
11. Marzetti E, Csiszar A, Dutta D, Balagopal G, Calvani R, Leeuwenburgh C. Role of mitochondrial dysfunction and altered autophagy in cardiovascular aging and disease: from mechanisms to therapeutics. *Am J Physiol Heart Circ Physiol*. 2013;305(4):H459-H476. doi:10.1152/ajpheart.00936.2012
12. Wu B, Yu L, Wang Y, et al. Aldehyde dehydrogenase 2 activation in aged heart improves the autophagy by reducing the carbonyl modification on SIRT1. *Oncotarget*. 2016;7(3):2175-2188. doi:10.18632/oncotarget.6814
13. Palikaras K, Lionaki E, Tavernarakis N. Mechanisms of mitophagy in cellular homeostasis, physiology and pathology. *Nat Cell Biol*. 2018;20(9):1013-1022. doi:10.1038/s41556-018-0176-2
14. Lazarou M, Jin SM, Kane LA, Youle RJ. Role of PINK1 binding to the TOM complex and alternate intracellular membranes in recruitment and activation of the E3 ligase Parkin. *Dev Cell*. 2012;22(2):320-333. doi:10.1016/j.devcel.2011.12.014
15. Okatsu K, Uno M, Koyano F, et al. A dimeric PINK1-containing complex on depolarized mitochondria stimulates Parkin recruitment. *J Biol Chem*. 2013;288(51):36372-36384. doi:10.1074/jbc.M113.509653
16. Peoples JN, Saraf A, Ghazal N, Pham TT, Kwong JQ. Mitochondrial dysfunction and oxidative stress in heart disease. *Exp Mol Med*. 2019;51(12):1-13. doi:10.1038/s12276-019-0355-7
17. Jiang M, Li X, Zhang J, et al. Dual Inhibition of Endoplasmic Reticulum Stress and Oxidation Stress Manipulates the Polarization of Macrophages under Hypoxia to Sensitize Immunotherapy. *ACS Nano*. 2021;15(9):14522-14534. doi:10.1021/acsnano.1c04068
18. El Manaa W, Duplan E, Goiran T, et al. Transcription- and phosphorylation-dependent control of a functional interplay between XBP1s and PINK1 governs mitophagy and potentially impacts Parkinson disease pathophysiology. *Autophagy*. 2021;17(12):4363-4385. doi:10.1080/15548627.2021.1917129
19. Cai H, Chen S, Liu J, He Y. An attempt to reverse cardiac lipotoxicity by aerobic interval training in a high-fat diet- and streptozotocin-induced type 2 diabetes rat model. *Diabetol Metab Syndr*. 2019;11(1):43. doi:10.1186/s13098-019-0436-8
20. Ren BC, Zhang YF, Liu SS, et al. Curcumin alleviates oxidative stress and inhibits apoptosis in diabetic cardiomyopathy via Sirt1-Foxo1 and PI3K-Akt signalling pathways. *J Cell Mol Med*. 2020;24(21):12355-12367. doi:10.1111/jcmm.15725
21. Liu Z, Nan P, Gong Y, Tian L, Zheng Y, Wu Z. Endoplasmic reticulum stress-triggered ferroptosis via the XBP1-Hrd1-Nrf2 pathway induces EMT progression in diabetic nephropathy. *Biomed Pharmacother*. 2023;164:114897. doi:10.1016/j.biopha.2023.114897
22. Vermot A, Petit-Härtlein I, Smith SME, Fieschi F. NADPH Oxidases (NOX): An Overview from Discovery, Molecular Mechanisms to Physiology and Pathology. *Antioxidants*. 2021;10(6):890. doi:10.3390/antiox10060890